

AMES GRANT
IN-24-CR
158848
178

A TEST FOR INTERFACIAL EFFECTS AND STRESS TRANSFER IN CERAMIC MATRIX COMPOSITES

NASA GRANT NAG 2-444

FINAL REPORT ✓

AUGUST 1, 1988

Prepared For
AMES Research Center
National Aeronautics and Space Administration
Moffet Field, CA 94035

From
Department of Materials Science and Engineering
University of Utah
Salt Lake City, Utah, 84112

(NASA-CR-182873) A TEST FOR INTERFACIAL
EFFECTS AND STRESS TRANSFER IN CERAMIC
MATRIX COMPOSITES Final Report (Utah Univ.)
17 p CSDL 11D

N88-29880

Unclas
G3/24 0158848

A TEST FOR INTERFACIAL EFFECTS AND STRESS TRANSFER IN CERAMIC MATRIX COMPOSITES

Dr. Willard D. Bascom (Research Professor)

Mr. Ilzoo Lee (graduate student)

1. INTRODUCTION

Fiber reinforced ceramic matrix composites are receiving considerable¹⁻³ attention for application in engines, as thermal protection materials, and for special electronic/electrical devices. The primary reason for the interest in these materials is the expectation that strong ceramic fibers can prevent catastrophic brittle failure in ceramics by providing various energy dissipation processes during crack propagation. Early work utilizing carbon fibers in ceramic matrices demonstrated the potential for this approach^{4,5}. However, carbon fibers are vulnerable to degradation in oxidizing reaction environments at relatively low temperatures; much below the use temperature of the ceramic materials. However, silicon carbide fibers (SiC) are more oxidation resistant than carbon fibers and are chemically compatible with many ceramic matrices.

Fiber-reinforcement of ceramics should, in principle, increase the resistance of the ceramic matrix. In general, this improved toughness has not been fully realized either because the fiber/matrix adhesion is too strong or too weak. The schematics in Figure 1 represents the load sharing (shear lag) for strong bonding (A) and weak bonding (B). If as in Figure 1A, the redistribution length is short then the overload on adjacent fibers is highly concentrated so that a single fiber break could initiate breaks in neighboring fibers*and catastrophic failure of the composite. On the other hand, if the shear stress at a fiber break is large enough to cause debonding some distance from the fiber end then load is distributed over a longer fiber length and is less likely to fracture adjacent fibers (Figure 1B). Clearly, there must be some optimum boundary strength. If the interfacial strength is too low there will be

* this effect has been recently demonstrated for carbon fibers in a polymer matrix using the embedded single filament test; "SURFACE AND INTERFACIAL PROPERTIES OF CARBON FIBERS," Progress Report NAG -1-706, W.D. Bascom Material Science and Engineering Department, University of Utah, June, 1988

excessive debonding and a loss in the strength of the composite compared to the unreinforced ceramic.

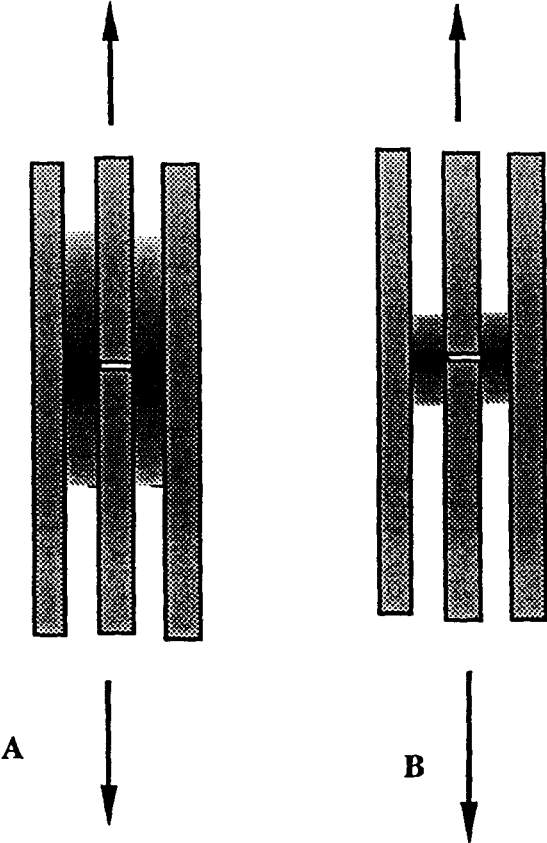


Figure 1 - Comparison of load sharing for weak fiber/matrix adhesion (A) vs strong adhesion(B).

However, there is a serious lack of information on shear lag effects in ceramic/matrix composites and how the properties of the fiber and the matrix influence stress distribution at fiber breaks. The factors which are expected to influence the properties of a fiber/matrix boundary (interphase) region are the mechanical properties of the components themselves, and the degree of physical and chemical interaction between the fiber and matrix. Clearly, the interphase properties are a major factor in the mechanics and environmental resistance of FRCM composites and there is a need to develop techniques to study this boundary region, especially the degree of adhesion.

Bascom et. al. ⁶ have successfully used microscale (25 mm gauge length) "dogbone" specimens with single carbon fiber embedded

through the length of each specimen as a method for determining the fiber/resin interphase strength for polymer matrix composites. A schematic of the single fiber test specimen adapted for ceramic matrix systems is shown in Figure 2. The work reported here originated from the idea that this technique could be applied to the fiber/ceramic matrix systems.

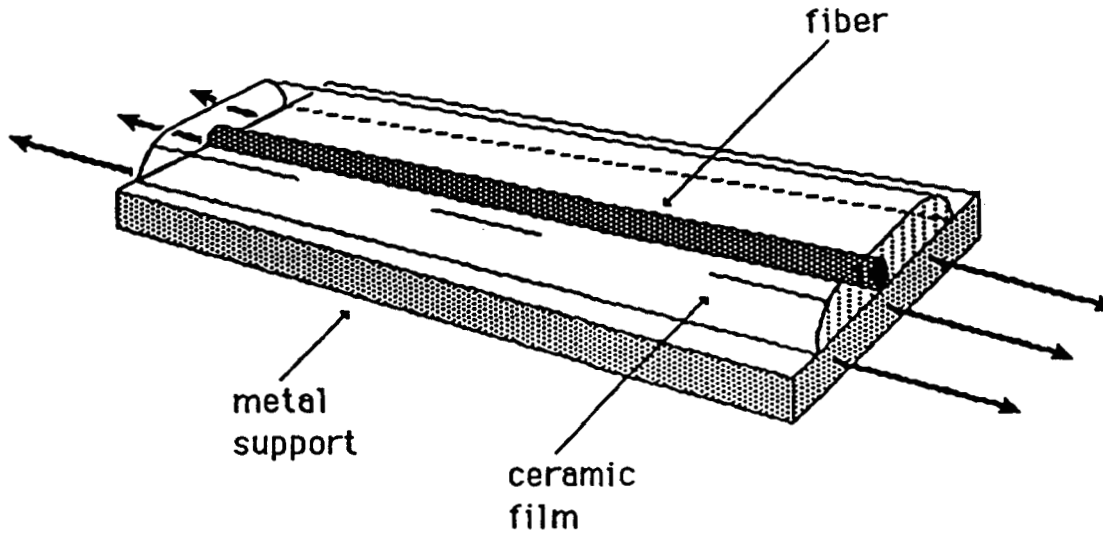


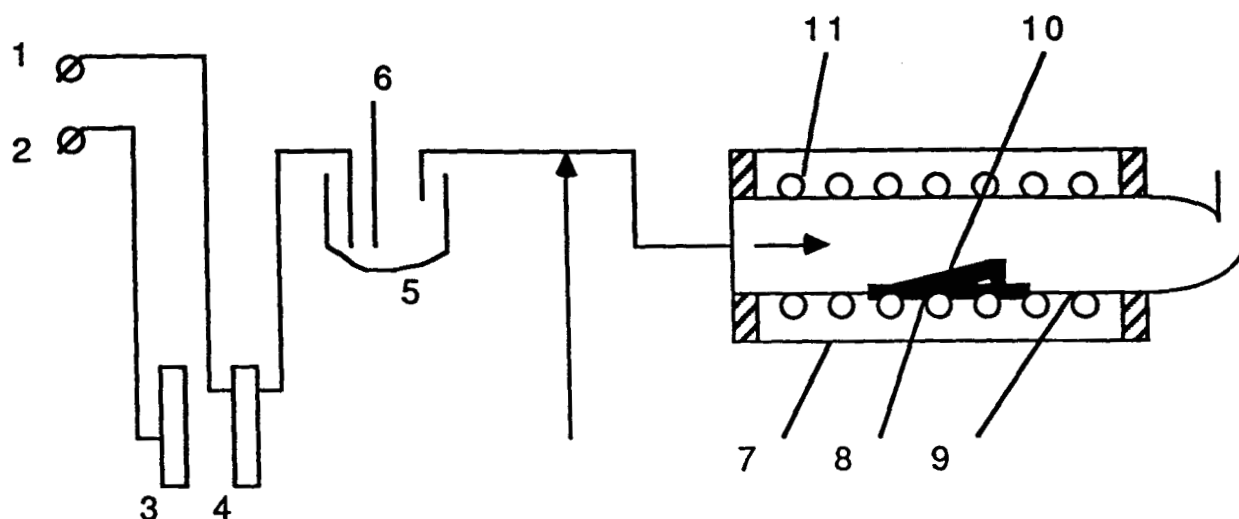
Figure 2 - Schematic of single filament specimen for adhesion testing

The purpose of this research program was to determine the feasibility of developing this test method to investigate the properties of the interphase between embedded fibers and ceramic matrices grown by chemical vapor deposition (CVD). The specific systems examined were carbon fibers and silicon carbide fibers embedded in silicon carbide.

II. EXPERIMENTAL PROCEDURE

Silicon carbide coatings were applied to three different pure metal substrates; Ni, W, and Mo having 99.995% purity. Table 1 summarizes the various properties of each metal. The substrates were cut (1.5 cm X 3.5 cm X 0.2 cm) using a low speed diamond saw and the surfaces polished using sand paper. In an experiment to determine the effect of substrate surface, a molybdenum plate was ground, polished and ion milled to a depth of 3000Å using an argon source. Ion milling removes any spurious contamination and heavy oxide layers.

An initial silicon carbide coating was produced from dimethyl-dichlorosilane (DMDCS) chemically deposited using a hot-wall horizontal silica tube reactor. Figure 3 shows a schematic diagram of the laboratory reactor use for the deposition of the coatings in this study. The DMDCS was injected into a manifold by bubbling through with argon gas, and was mixed with and carried by hydrogen into the reaction chamber. The total flow rate was kept constant between 0.2-0.3 mole/hour, and the pressure of the reactor was maintained at 1atm throughout this study.



- | | |
|-----------------------|---------------------|
| 1. Argon Cylinder | 8. Silica Boat |
| 2.. Hydrogen Cylinder | 9. Silica Tube |
| 3,4 Rotameter | 10. Metal Substrate |
| 5. Bubbler | 11. Heating Element |
| 6. Thermometer | |
| 7. Furnace | |

Figure 3 Schematic Diagram of Laboratory Reactor

The substrates were preheated to the deposition temperature and maintained in a flow of hydrogen for a minimum of 10 minutes prior to each deposition run. The substrate temperatures ranged

from 1040 to 1060°C measured by means of a thermocouple at the substrate. One of the problems of the horizontal reactor is the depletion of the reactant in the downstream direction which results in a gradient in film thickness along the substrate⁷. This effect was partially corrected by slightly tilting the substrates, thus diminishing the effective cross section of the reactor.

When the first layer of silicon carbide coating (~20µm) was applied, the sample was slowly drawn from the reactor to ambient temperature using a silica rod. This procedure was used for all of the silicon carbide depositions.

Two different fibers, carbon and Nicalon SiC, were obtained from Hercules Aerospace and NASA-Ames respectively and their typical properties are summarized in Table II and III. A single fiber was positioned lengthwise on top of the first layer of silicon carbide (the undercoating) by using a high temperature paste (Sauereisen). The fiber was overcoated by growing another silicon carbide layer using the same conditions as for the first layer. The thickness of the deposited silicon carbide layer was determined by comparing the diameter of uncoated Nicalon SiC fiber with the deposited layer.

The crystalline phases present in silicon carbide depositions were identified by X-ray diffraction using CuK radiation.

III. RESULTS and DISCUSSION

The two principle results of this study were the profound effect of differences in the thermal coefficient of expansions of the substrate, silicon carbide matrix and fiber on the preparation of the test specimen and secondly, the formation of a brittle zone at the substrate /matrix interphase. Indeed, differential thermal stresses generally prevented the fabrication of useful specimens and in the case where a reasonable system was found, the formation of a brittle zone between matrix and substrate prohibited any meaningful measurements.

Initially, nickel plates was used as substrates. The undercoating was uniform in terms of X-ray analysis. Optical micrographs of a silicon carbide undercoating on nickel substrate are shown in Figure 4. The deposits are fairly smooth and the surface of the substrate was completely covered with a film having an approximately equal ratio of pentagonal and hexagonal grains.

However, placement of the carbon fiber followed by further CVD produced a coating with cracks and a tendency to peel from the substrate. Evidently, the severity of the stresses in the coating increase prohibitively with coating thickness. Figure 5 shows the optical micrograph of cracks and peeling of the coating and resulting damage of the fiber. The primary reason for the peeling of the coating is the thermal expansion coefficient mismatch ($\Delta = 10.2 \times 10^{-6}/\text{K}$) between the nickel substrate and the grown silicon carbide coating. Furthermore, the carbon fiber positioned lengthwise showed a number of breakages due to a large thermal expansion coefficient mismatch between the nickel substrate and carbon fiber and to possible chemical attack on the fiber by the gas phase components used in the CVD process.

Since SiC fibers are more stable at high temperature and in the CVD gas phase than carbon fibers, Nicalon SiC fiber was used in subsequent experiments. In addition tungsten and molybdenum substrates were used in place of nickel since their thermal expansion coefficients do not differ appreciably from that of silicon carbide ($\Delta = 1.5 \times 10^{-6}/\text{K}$ and $2.0 \times 10^{-6}/\text{K}$ for tungsten and molybdenum, respectively). When the tungsten substrate was used, the overcoating of the SiC fiber was successful except for minor peeling of the coating at the edges of the substrate. However, during the coating process, the tungsten became very brittle presumably due to H_2 in the gas mixture which is necessary to obtain a high quality silicon carbide coating. This embrittlement of the substrate caused technical difficulties in testing the sample; the sample shattered into brittle platelets when it was gripped in the microtensile test unit. When the molybdenum substrate was used, however, better adhesion of the SiC coating was obtained and there was less embrittlement of substrate by the hydrogen. Ion milling of the molybdenum substrate resulted in even better adhesion of the coating compared to the unmilled, abraded substrate. Figure 6 shows a scanning electron micrograph of a cross section of the sample of a SiC fiber in silicon carbide on molybdenum. A continuous coating from the substrate to the overcoating on the fiber is clear. However, there is a evidence of some reaction products between the silicon carbide and the molybdenum. Figures 7 and 8 compare scanning electron micrographs of the naked fiber and the silicon carbide coated fiber. The characteristic "corn cob" surface of chemically vapor deposited silicon carbide fiber is seen in Figure 8. Figure 9 shows the overcoated SiC fiber after four hours of coating time. It is seen that homogeneous layers adhere well to the fiber surface over the length and perimeter of the fiber. However, the fiber was

not completely embedded in this short time but was fully covered after ten hours. Figure 10 shows complete embedment of the fiber. Scanning electron micrographs of the fractured cross section of this sample are shown in Figure 11. They clearly show the embedding of the SiC fiber by the grown silicon carbide layers. However, there is also evidence of poor adhesion of the coating to the substrate. The photograph suggests the formation of an interlayer. However, the debonding could have been simply due to stresses in the silicon carbide coating.

The crystalline phases present in SiC deposited at 10500C in these experiments with molybdenum substrates were identified using X-ray diffraction (Ni filtered CuK). Representative X-ray diffraction patterns of the sample are shown in Figure 12. Only three distinguishable peaks were detected. The strongest lines corresponding to the (111) reflection of SiC was observed in the diffraction pattern. The sample consisted predominantly of the β -phase of SiC. There was no X-ray evidence for silicon which is usually observed in low temperature deposition¹⁰.

IV CONCLUSIONS

The efforts to fabricate single embedded filament specimens of carbon and SiC fibers were unsuccessful largely due to the thermal stresses resulting from differences in thermal coefficient of expansion. Other factors appear to have been involved including embrittlement of the metal substrate by the H₂ gas in the CVD flow stream and reaction layers formed between the silicon carbide and the metal substrates. The carbon fiber may have been attacked by the CVD reactant.

It is our conclusion that these differential stresses are so large as to make the embedded fiber test impractical for the study of interphase effects and stress transfer in fiber/ceramic matrix systems. Even when the fiber and coating were identical, SiC, the stresses built up in the silicon carbide layer at thicknesses comparable to that of the fiber (a necessary condition for this test technique) resulting in cracking and peeling of the coating even when the thermal coefficients of expansion of the coating and substrate were very small as was the case for silicon carbide on molybdenum. Moreover, even if intact specimens could be prepared, the residual stress in the coating would make interpretation of the test results (fragmentation of the filament under tensile loading⁶) prohibitively difficult. Certainly, the test would not be generally

applicable but would be limited to fiber/matrix (and substrate) materials with similar if not identical α .

V RECOMMENDATIONS

Alternative methods of investigating the interphase region in ceramic matrix materials should be considered. The microindentation "push out" test is a likely candidate if the push-out force is measured as a function of specimen thickness so that the frictional adhesion can be distinguished from interphase fracture¹¹. This approach is less ambiguous than simply measuring the indentation force and displacement¹².

Micro-indentation tests have been largely limited to the study of relatively large fibers such as the silicon carbide coated boron filaments. However, advanced techniques and equipment have become available that can be applied to samples with small diameter (<20 μ m) fibers. Much of the hardware for ultra-micro (nano) indentation has been developed for the rapidly advancing field of scanning tunnelling and atomic force microscopy (STM &AFM). Although the commercial test equipment for nano-indentation testing is very costly, much of this cost is for peripheral devices. The nano-positioner is relatively inexpensive to construct and the techniques for producing micro stylus indenters have been improving steadily* . Observation of the specimen, even for carbon fibers with diameters of 5 μ m can be made using simple light microscopy.

* ion-milling methods of producing < nm diameter stylus tips for STM and AFM have been developed at the University of Utah, Center for Biopolymer Interfaces.

VI. REFERENCES

1. E. Fitzerand and R. Gadow, " Fiber Reinforced Silicon Carbide", Am. Ceram. Soc. Bull., 65, 326 (1986)
2. J. A. Cornie, Y. M. Chiang, D. R. Uhlman, A. Mortensen, and J. M. Collins, "Processing of Metal and Ceramic Matrix Composites", Am. Ceram. Soc. Bull., 65, 293 (1986)
3. E. C. Luh and A. G. Evans, "High Temperature Mechanical Properties of a Ceramic Composites", J. Am. Ceram. Soc., 70, 466 (1987)
4. R. A. Sambell, D. H. Bowen, and D.C. Phillips, "Carbon Fiber Composites with Ceramic and Glass Matrices, Part 1, Discontionuous Fibers", J. Mater. Sci., 7, 663 (1972)
5. R. A. Sambell, et. al., " Carbon Fiber Composites with Ceramic and Glass Matrices, Part 2, Continuous Fibers", *ibid*, 7, 676 (1972)
6. W. D. Bascom and R. M. Jensen, "Stress Transfer in Single Fiber/ Resin Tensile Tests", J. Adhesion, 19, 219 (1986)
7. W. Kern and V. S. Ban, "Chemical Vapor Deposition of Inorganic Thin Films " in Thin Film Processes edited by J. L. Vossen and W. Kern, Academic Press, 25 (1978)
8. K. K. Chawla, "Composite Materials-Science and Engineering", Spriger-Verlag, 37-57 (1987)
9. G. Verspui, "CVD of Silicon Carbide and Silicon Nitride on Tools for Electrochemical Machining" in Proc. of the Seventh International Conference on Chemical Vapor Deposition edited by T. O. Sedgwick et. al.", 463 (1979)
10. T. D. Gulden, " Deposition and Microstructure of Vapor-Deposited Silicon Carbide", J. Am. Ceram. Soc., 8, 424 (1968)
11. D. K. Shetty, "Shear-Lag Analysis of Fiber Push-Out Tests for Estimating Interfacial Friction Stress in Ceramic Matrix Composites", J. Am. Ceram. Soc. , 71, C107 (1988)
12. D. B. Marshall and W. C. Oliver, "Measurement of Interfacial Mechanical Properties in Fiber-Reinforced Ceramic Composites," J. Am. Ceram. Soc., 70, 542 (1987)

Table 1 Physical properties of metal substrates

	Ni*	W**	Mo**
Melting Point(°C)	1453	3387	2610
Linear Exp. Coef. (10 ⁻⁶ /°k) (at 20°C)	13.3	4.6	5.1
Crystal Structure	FCC	BCC	BCC

Sources: * Good Fellow Metals Cambridge Ltd, Cambridge, England

** , Alpha Products, Danvers, Massachusetts

Table 2 CARBON FIBER PHYSICAL PROPERTIES+

Density (gm/cm ³)	1.83
Diameter (µm)	6-7
Modulus (GPa)	230
Strength (GPa)	3.5
Linear Expansion Coefficient (10 ⁻⁶ /°k)	-0.1-0.5

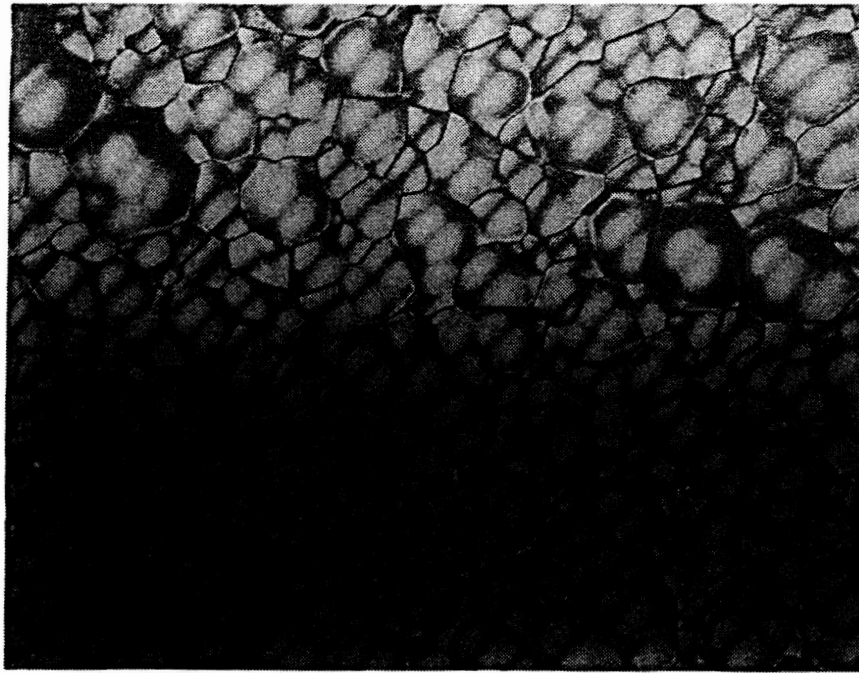
+ AS4, Hercules Aerospace, Magna, Utah

Table 3 Nicalon SiC⁺⁺ fiber physical properties

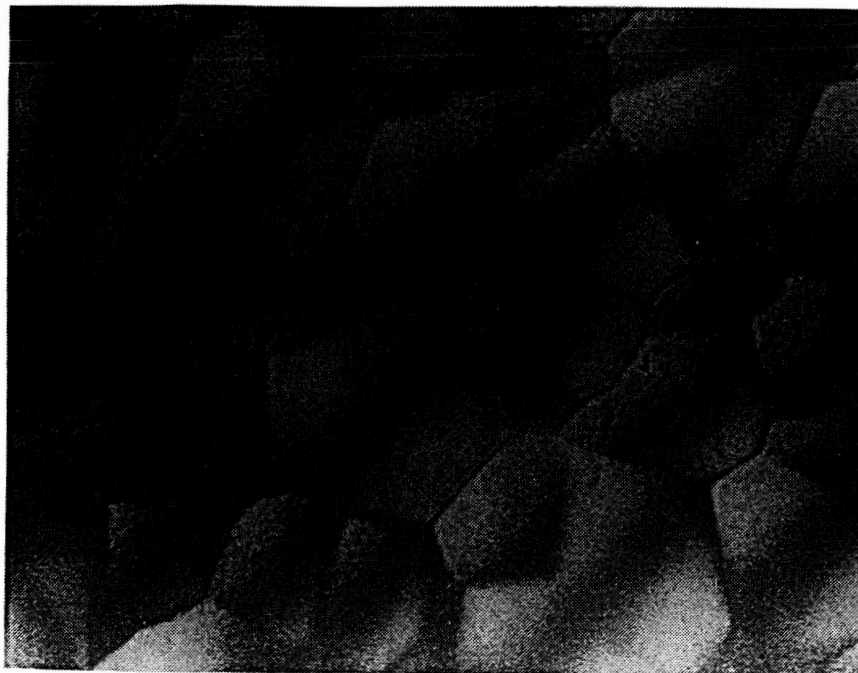
Density (gm/cm ³)	2.6
Diameter (μm)	10-20
Modulus (GPa)	180
Linear Exp. Coef. (10 ⁻⁶ /°k)	3.1
Strength at 20°C (GPa)	
As-Produced	2
After 1400°C (argon)	<1
Strength at 1400°C (oxygen)	<0.5
Creep Strain at 1300°C, 0.6GPa, 20h (%)	4.5

++ NASA-AMES Research Center, Moffet Field, California

ORIGINAL PAGE IS
OF POOR QUALITY.



63 μ m



25 μ m

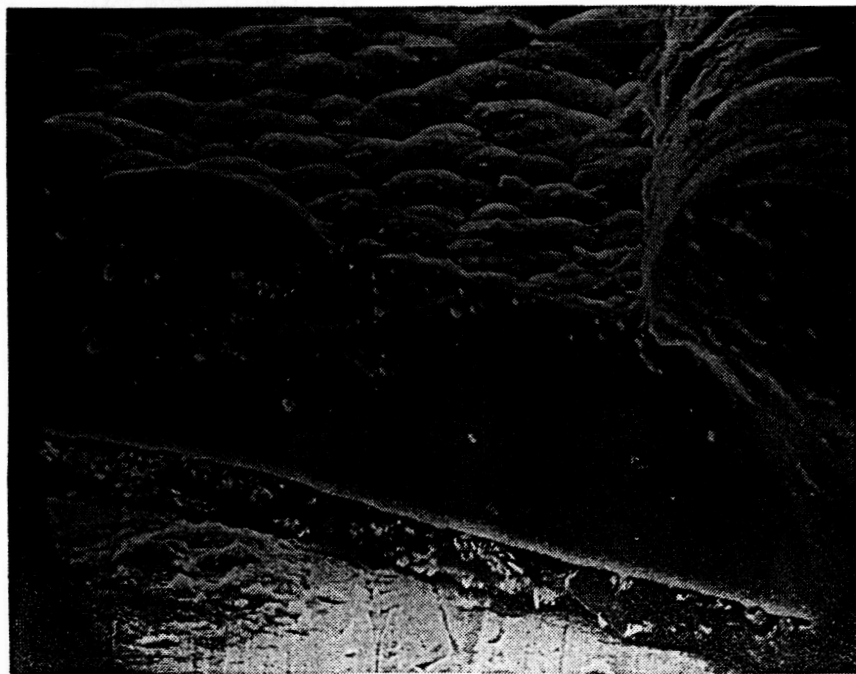
Figure 4 Optical micrographs of a silicon carbide undercoating
on Nickel substrate

ORIGINAL PAGE IS
OF POOR QUALITY



50 μm

Figure 5 Optical micrograph of cracks and peeling of the coating



10 μm

Figure 6 SEM photograph of a cross section of a sample

ORIGINAL PAGE IS
OF POOR QUALITY

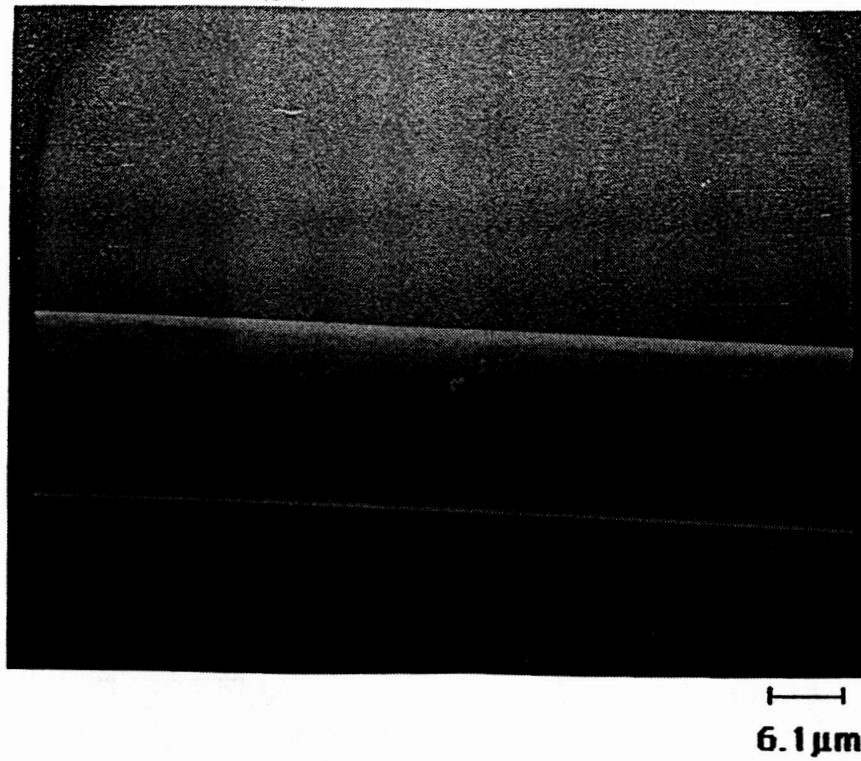


Figure 7 Uncoated Nicalon SiC Fiber

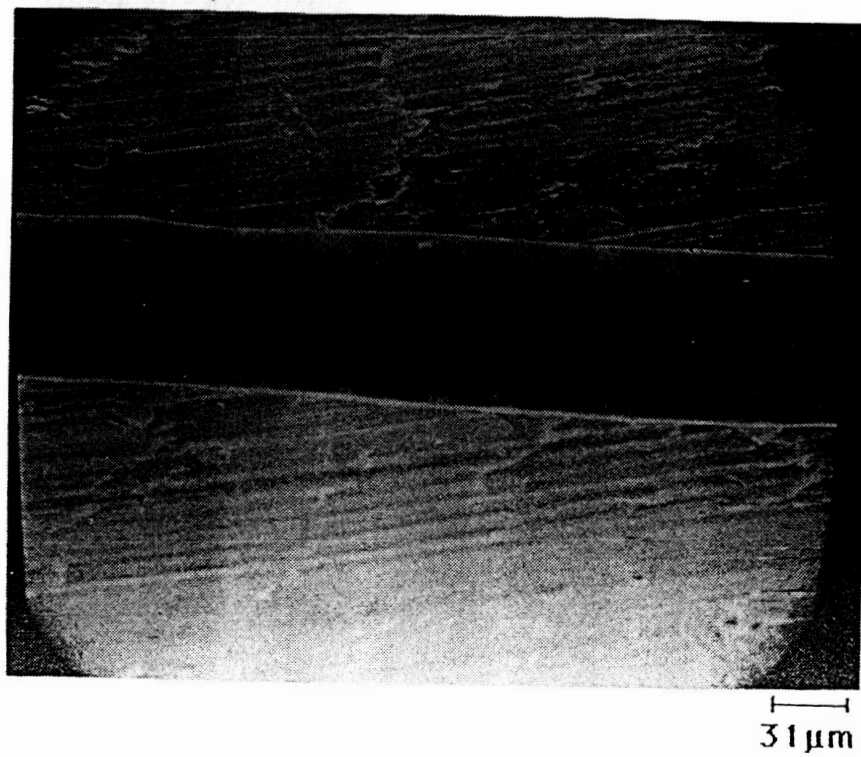


Figure 8 CVD coated Nicalon SiC fiber

ORIGINAL PAGE IS
OF POOR QUALITY

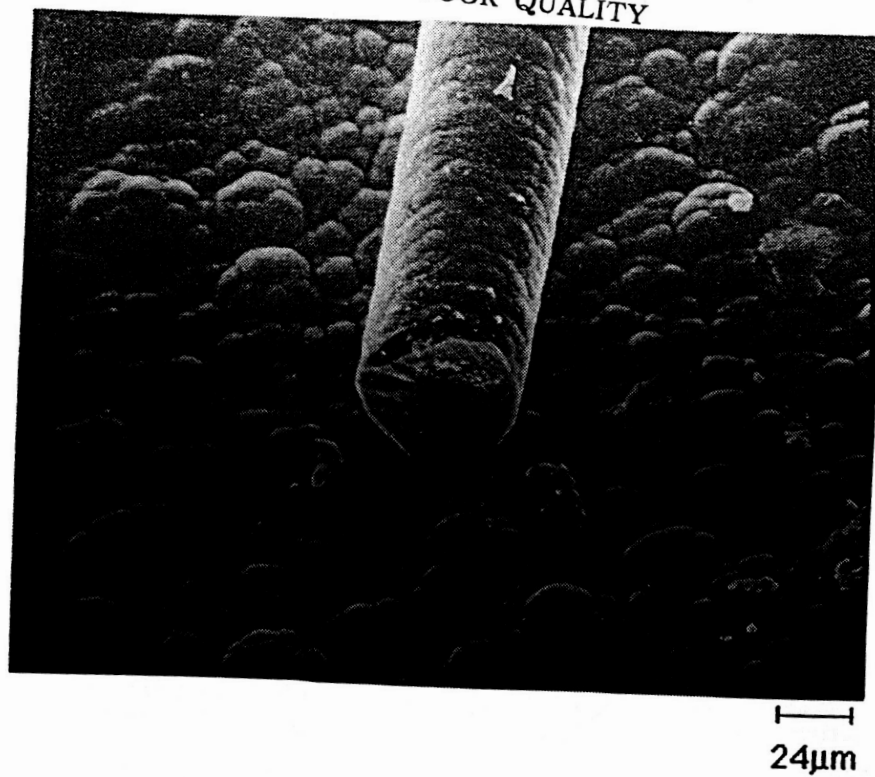


Figure 9 Overcoated SiC fiber after 4 hours coating time

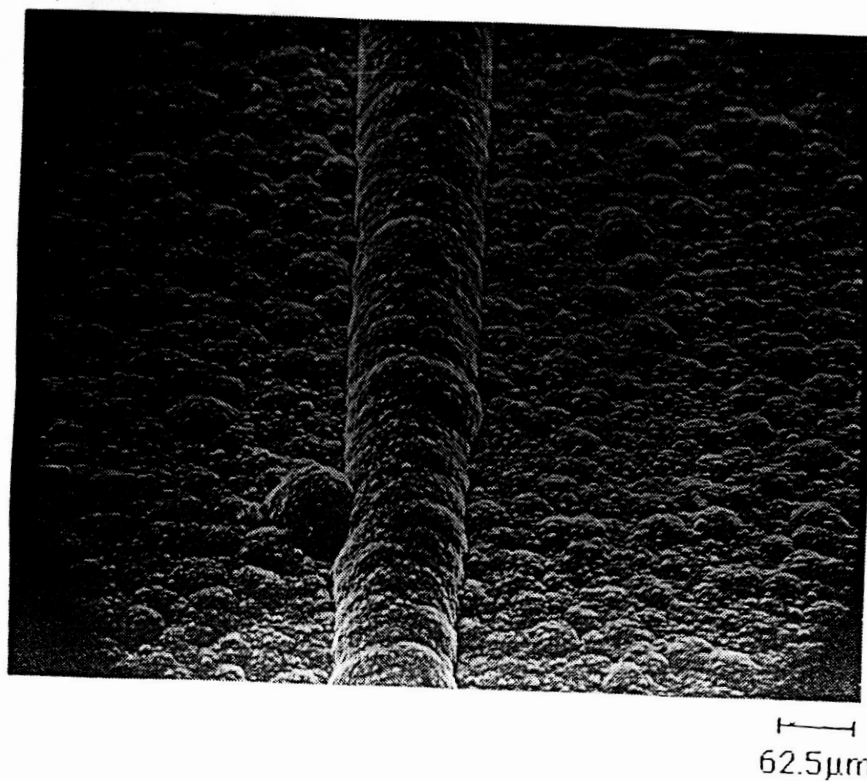
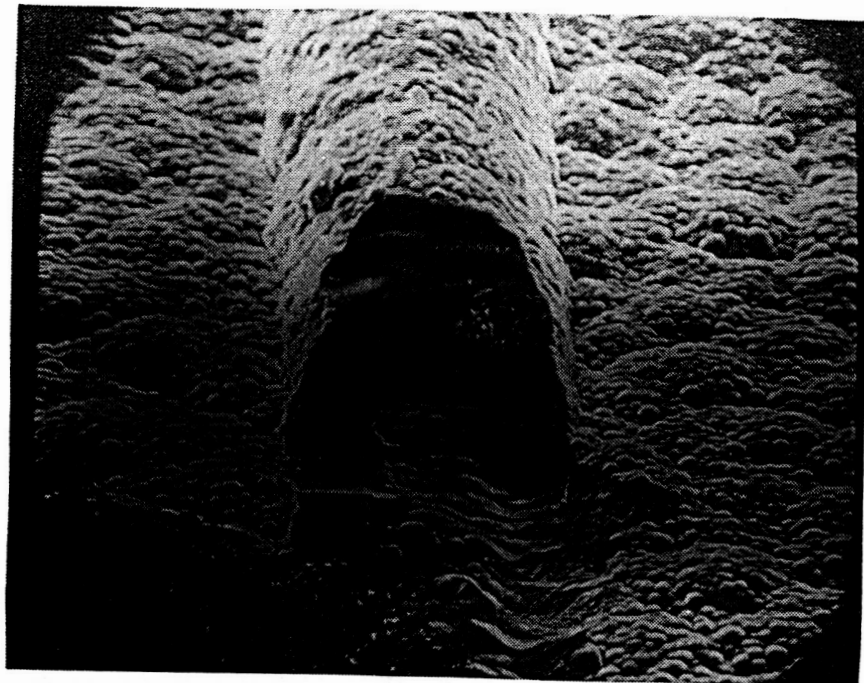
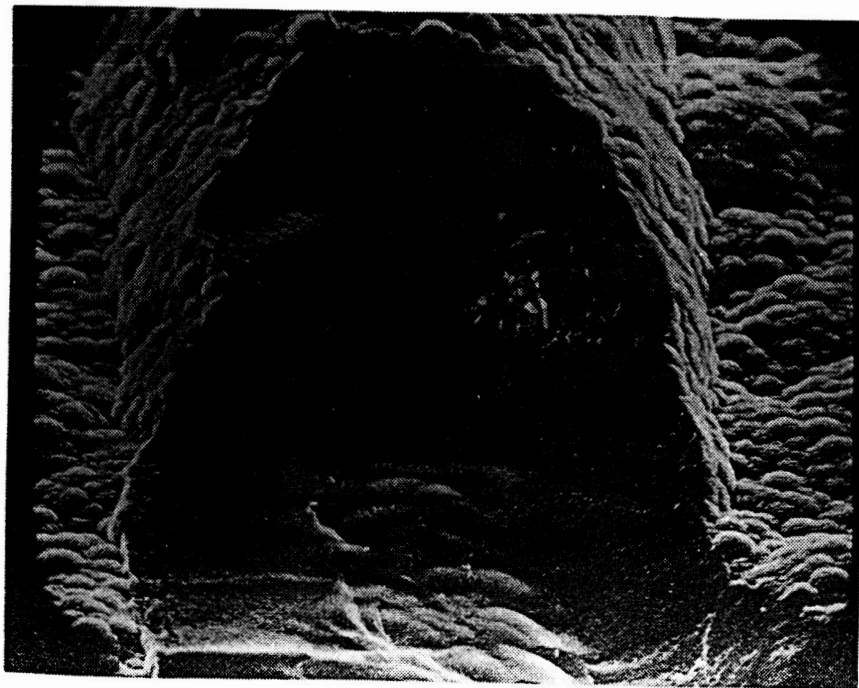


Figure 10 Overcoated SiC fiber after 10 hours coating time

ORIGINAL PAGE IS
OF POOR QUALITY



—|—|
25 μ m



—|—|
12.5 μ m

Figure 11 Scanning electron micrographs of fractured cross section